MOTIONS OF PEBBLES ON PEBBLE BEACH

Ichiro Deguchi[1], Masanobu ONO[1], Susumu ARAKI[1] and Toru SAWARAGI[2]

ABSTRACT

Motions of pebbles on an artificial pebble beach were measured by tracking tracers. After the beach profile reached equilibrium, pebbles moved mainly in the longshore direction parallel to the shore line under the condition of oblique wave incidencc. Intensive motions of pebbles were observed in the swash zone and the maximum displacement reached 30m during one week. The authors proposed a numerical procedure for analyzing pebble motion. The motion of pebble up to the maximum wave set-up point can be predicted numerically when the time and spatial variation of water particle velocity and fluid force on pebbles are given.

INTRODUCTION

The authors have been carrying out series of field studies on an artificial pebble beach constructed as a seawall of the reclamation. The sea wall was originally designcd as a usual vertical seawall with wave energy absorbing blocks in front of it. However it was altered to be a permeable gentle slope seawall constructed by using pebbles of marble. The reason was that the mild slope permeable seawalls has little influence on the surrounding coast. The accessibility to the shoreline is also greatly improved when compared with the impermeable seawalls with armor blocks.

A gentle slope seawall is usually constructed by using rubble stones with a cover layer. Therefore any significant deformation of the cover layer is not permitted in the design because the deformation may cause fatal destruction of the seawall. The artificial pebble beach was constructed without cover layer and the dcformation in the profile is permittcd as far as it maintains the initially designed hydraulic function as is the casc of the artificial sandy beach. Therefore it is necessary to know the deformation pattern of the beach and the change in the hydraulic function caused by the deformation. Although a number of research has already been done about the deformation of sandy beach, only a few have been done on the pebble beach.

In this paper movement of pebbles on the artificial pebble beach is investigated through field measurement of the motion of pebbles. Numerical model for analyzing the movement of pebbles is constructed to know the influence of the geometry of the beach, diameter of the pebble and characteristics of incident waves on the pebble motion.

1 Prof., Lecturer and Student of Graduate School, Dept. of Civil Eng., Osaka University, Yamada-oka, Suita-city , Osaka 565, Japan
2 Prof., Dept. of Civil Eng., Osaka Sangyo University, Daito-city Osaka, Japan

FIELD MEASUREMENT OF PEBBLE MOTION

Figure 1 shows the location and plane view of the artificial pebble beach. The total length of the beach is about 3 km and the slope of the beach is 1/15. A representative cross section of the beach is schematically illustrated in Fig.2. The beach was constructed by rubbles of a mean diameter about 6 cm and covered by the pebble of marble of the diameter 4 to 8cm. The thickness of marble layer is about 1m. The beach is divided into some portions by groins of the length about 80m. The length of the beach of one portion is 300m.

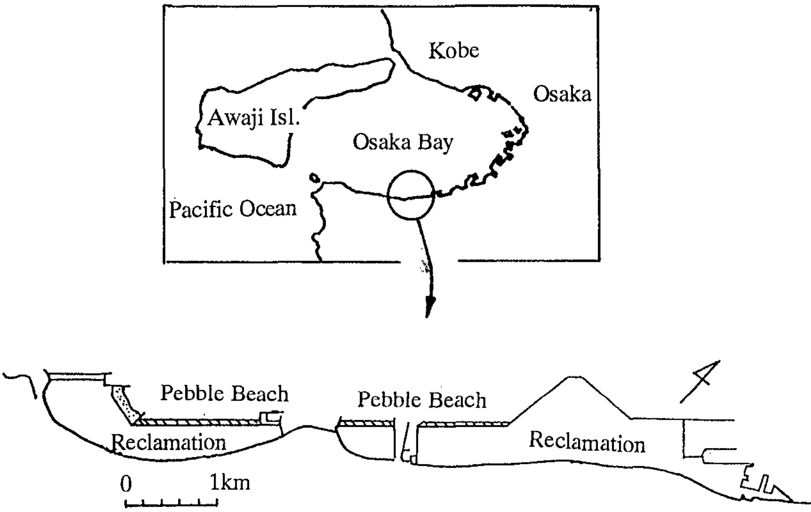

Fig. 1 Location and plane view of the artificial pebble beach

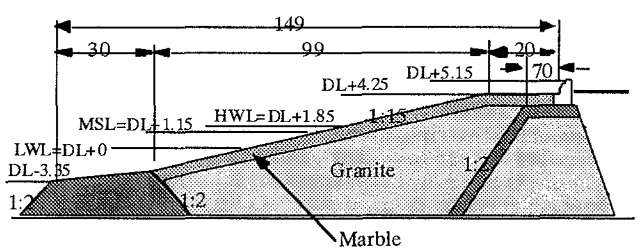

Fig 2 Representative cross-section of the pebble beach

Figure 3 is the bottom topography of the objective beach measured on November 1996. The predominant wave direction is found to be vary from season to season but waves from north and northwest predominant all through the year. The cross-shore profile reached equilibrium relatively shortly after the completion and longshore movement of the pebble from SW to NE. As a result, contour lines advanced more than 15m around measuring lines Nos. 13 and 15. (Deguchi et al, 1996)

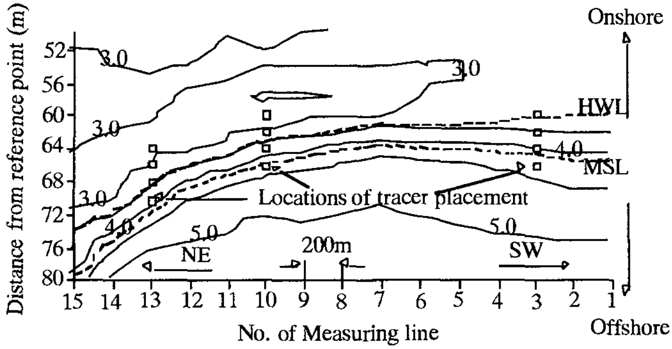

Fig.3 Bottom profile of the objective beach (Nov., 1997)

Until 1997 we carried out four times measurements of the pebble motion on the beach. Here the results of the first two measurements are analyzed. In the measurement, pebble motions were measured by tracking pebbles to which running number were given. 10 to 20 numbered pebbles were placed at four locations at the distance of 2 m along the three measuring lines perpendicular to the initial shoreline. The displacements of pebbles were measured one week after the placements.

The first measurement was conducted during 21st and 28th of November 1996. Tracers were placed along the measuring lines Nos.3, 10 and 13 as shown in Fig.3. The south groin shades a region around the measuring line No.3 from the predominant incident waves. The longshore pebble transport due to the predominant incident waves becomes the maximum around measuring lines Nos.9 to 10 and the measuring line No.13 locates in the accretion area by the longshore pebble transport (Deguchi et al. 1996).

Figure 4 is the cross-section along the measuring line Nos.3, 10 and 13 where the tracers were placed at the first measurement. The most of tracers were placed above the MWL.

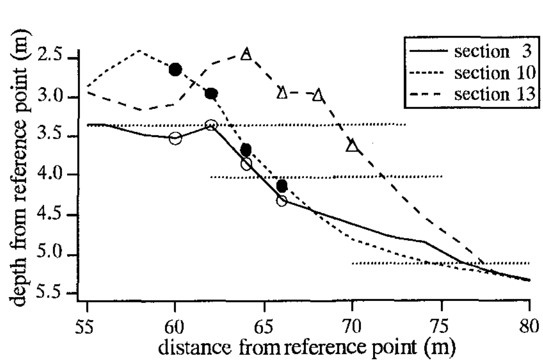

Fig. 4 Cross sections of tracer placement (First measurement)

The second measurement was carried out during 28th February and 7th March, 1997 just after finishing the maintenance reshape of the beach. The beach profile was reshaped to be an almost initial profile. Tracers were place along the measuring line Nos.5, 9 and 13.

The most of tracers except for the measuring line No.5 were placed between HWL and MWL as shown in Fig. 5.

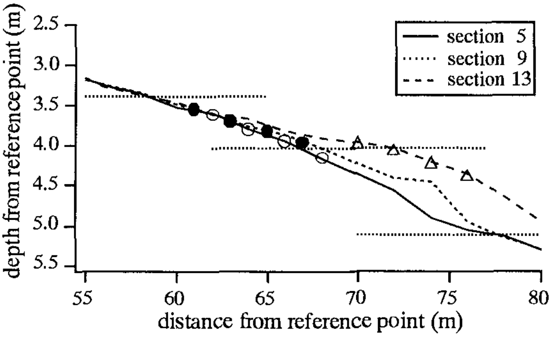

Fig. 5 Cross section of tracer placement (Second measurement)

CHARACTERISTICS OF INCIDENT WAVES AND MEADURED PEBBLE MOTIONS

First measurement:

Along the measuring line No.3 any movement of tracers could not be found and the tracers placed in the region higher than 2.8m along the measuring lines Nos.9 and 13 did not move. Figure 6 shows the measure displacements of tracer pebbles. More than 60% of the tracers placed along the measuring line No.9 were found.

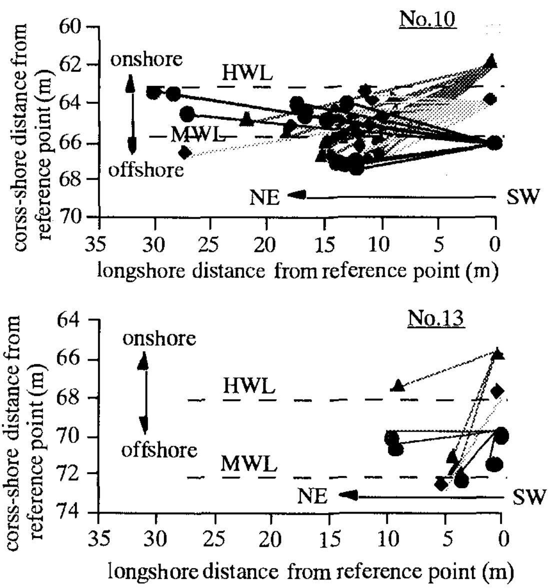

Fig. 6 Measured displacement of tracers along measuring line Nos.10 and 13 (first measurement)

All tracers moved in the longshore direction toward NE and the maximum longshore displacement is more than 30m. While the cross shore displacement was 4m at the maximum. As was already explained, the longshore pebble movement became the maximum around the measuring line Nos.9 and 10.

Only a few tracers placed along the measuring line No.13 were found They also moved in the longshore direction toward NE with the offshore displacement. The bottom profile was almost equilibrium around measuring line No.13 and the longshore pebble transport decreased to a large extent. It seemed that the a large part of tracers were covered by the pebbles transported in a steady stream from SW.

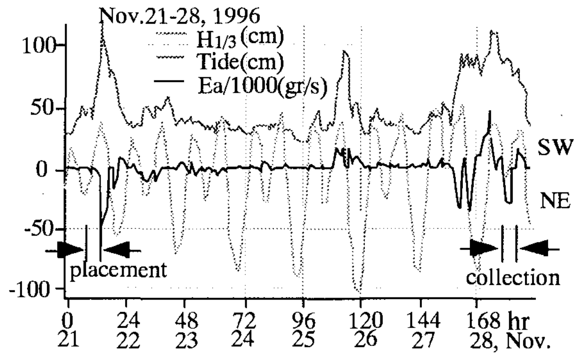

Fig.7 Incident waves and tidal level during the first measurement

Figure 7 is the time history of the incident waves and tidal level during the first measurement. A so-called E_a parameter that is usually used to relate incident waves and longshore sediment transport rate and is calculated from Eq.(1) are also shown.

$$E_a = \frac{1}{8}\rho g H^2 C_g \sin\theta\cos\theta \tag{1}$$

Just after the placement of the tracers, height of incident waves increased rapidly and finally it became more than 1 m. The direction of incident wave energy flux was from SW to NE. Active motion of tracers were observed under these waves. Another high waves of significant wave height more than 0.5m were measured in 25, 27 and 28 of November. Especially, during 27 and 28 high waves continued for more than 24 hrs and direction of incident wave energy in the period changed from NE to SW. In average incident wave energy flux from SW to NE was predominant in this period.

Second measurement:

In the second measurement, tracers placed in the deeper region along the measuring line No.5 did not move. Someone threw tracers in the shallower region. So, we could not judge whether the tracers were moved by waves or not.

Figure 8 is the measured displacements of the tracers along measuring lines Nos.9 and 13. Tracers placed in the deeper region than MWL moved longshore direction from NE to SW. However, the displacement was only 2m at the maximum. Tracers in the shallower region along measuring line No.9 moved little and tracers in shallower region along No.13 moved toward NE. The maximum displacement was 1m. More than 80% of the tracers were collected.

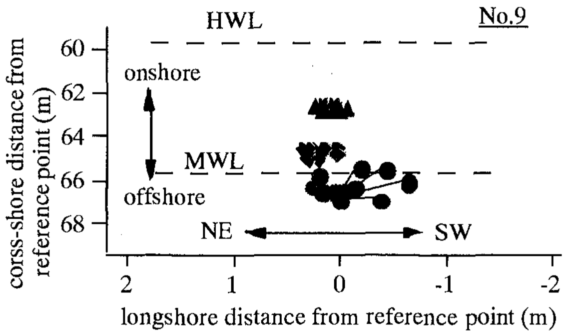

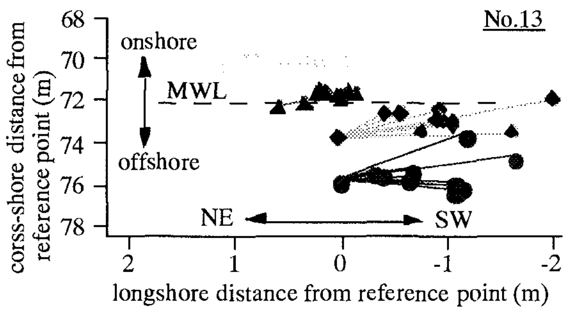

Fig. 8 Measured displacement of tracers along measuring line No.9 and 13 (Second measurement)

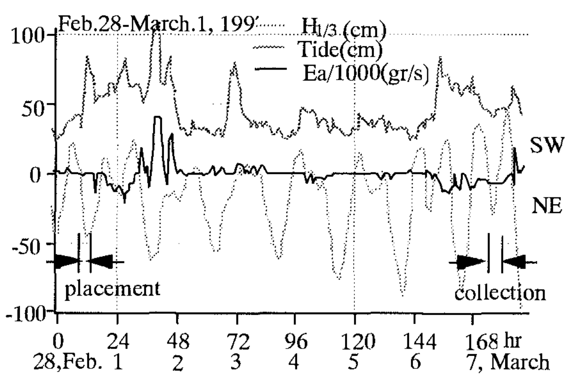

Fig.9 Incident waves and tidal level during the second measurement

Figure 9 is the time variation of significant incident waves, tidal level and value of E_a parameter. Large waves of wave height higher than 1m appeared only once when the tide was low. The energy flux was in the direction of SW. The movements of pebbles in the deeper region along Nos.9 and 13 were caused by these waves. Pebble motion in the shallower region might be caused by the waves of wave height higher than 0.5m and tide was high, i.e. 1 March and 6 March.

ANALYSIS OF PEBBLE MOTION

Modeling of pebble motion:

Currently there are two methods for analyzing pebble motion. One is a so-called discrete element method where the motions of all pebbles in an objected region are solved simultaneously (for example Araki et al.,1997). The other is the usual way to solve equations of motion for sliding and rotation of projected pebbles on the bottom. In this paper, the motion of pebble is analyzed by the latter method.

Here we focus on the motion of the projected pebble on the bottom. Figure 10 is the rough flow of our procedure for calculating motion of pebbles on the pebble beach. First of all we have to evaluate spatial and temporal variation of fluid motion in the objective region. This is done by calculating wave transformation and wave-induced current. Then fluid force on the projected pebble is estimated to determine the mode of motion and displacement of pebble. The loop is iterated during the desired time. The mode of the pebble motion and displacement of the pebble is determined by the equations of motion for rotation and sliding of pebble.

Spatial and temporal variation of fluid motion

⇩

Evaluation of fluid force on pebble

⇩

Determination of mode of pebble motion

⇩

Calculation of pebble displacement

⇩

Determination of mode of pebble motion

⇩

Calculation of pebble displacement

Fig. 10 Flow of calculation

Definition of the forces on the model pebble C whose diameter is a, mass in the air is W is shown in Fig.11 where X and Z are the displacements in the cross-shore and upward directions, v is the speed of the motion and ϕ is the mean bottom slope.

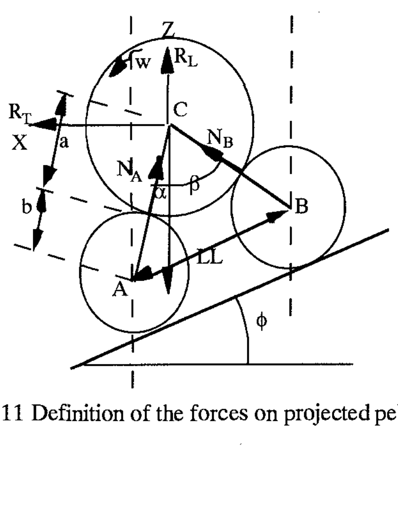

Fig.11 Definition of the forces on projected pebble

Horizontal and vertical fluid force are expressed by R_T and R_L and reactive forces from pebble A and B of diameter b are N_A and N_B. These forces are expressed by the following equations.

$$N_A = \frac{\left(W_g - R_L\right)\tan\beta + R_T}{\sin\alpha + \tan\beta\cos\alpha} \tag{2}$$

$$N_B = \frac{\left(W_g - R_L\right)\tan\beta + R_T}{\sin\beta + \tan\alpha\cos\beta} \tag{3}$$

When both N_A and N_B are positive, C dose not move. When N_A is positive and N_B is less than or equal to zero, pebble C moves toward left hand side and so on.

When the pebble moves toward left hand side as shown in Fig.12, the equations of motion are expressed by Eqs.(4)-(6).

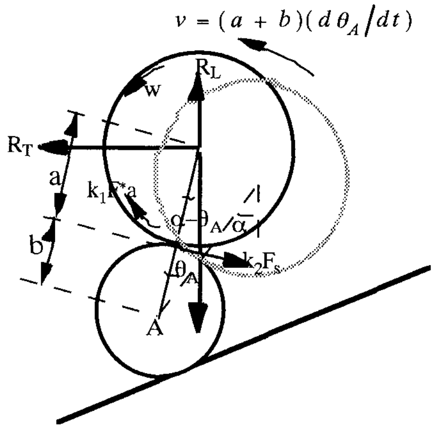

Fig.12 Motion of pebble to left hand side caused by rotation and sliding

Equation of motion in the horizontal direction:

$$M\frac{dv}{dt} = R_T\cos\left(\alpha-\theta_A\right) + \left(R_L - W_g\right)\sin\left(\alpha-\theta_A\right) + k_2F_S \tag{4}$$

Equation of motion in the upward direction:

$$M\frac{v^2}{a+b} = -R_T\sin\left(\alpha-\theta_A\right) + \left(R_L - W_g\right)\cos\left(\alpha-\theta_A\right) + N_A \tag{5}$$

Equation of motion of rotation:

$$I\frac{dw}{dt} = k_1F^*a - k_2F_Sa \tag{6}$$

where $I = \frac{2}{5}Ma^2$, M is the immersed mass of pebble C, θ_A is the displacement angle defined in Fig12 and the values of k_1 and k_2 are determined according to the direction of pebble motion as follows:

$$w \geq 0 : k_1 = 1, w \leq 0 : k_1 = -1 \tag{7}$$

$$v \geq 0 : k_2 = -1, v \leq 0 : k_2 = 1 \tag{8}$$

In this case, the speed of pebble motion v is expressed by Eq.(9)

$$v = (a+b)\frac{d\theta_A}{dt} \tag{9}$$

Using Eq. (9), Eqs.(4) to (6) are rewritten as follows:

$$M(a+b)\frac{d^2\theta_A}{dt^2} = R_T\cos(\alpha - \theta_A) + (R_L - W_g)\sin(\alpha - \theta_A) + k_2F_S \tag{10}$$

$$M(a+b)\left(\frac{d\theta_A}{dt}\right)^2 = -R_T\sin(\alpha - \theta_A) + (R_L - W_g)\cos(\alpha - \theta_A) + N_A \tag{11}$$

$$\frac{2}{5}Ma^2\frac{dw}{dt} = k_1F^*a - k_2F_Sa \tag{12}$$

$$f(t, \theta_A, F_S)\ ,\ g(t, \theta_A, N_A)\ ,\ h(t, w)$$

There are six unknowns in these equations, i.e.., N_A, θ_A, v, F_S, F^* and w. However, there are only five equations, i.e.., Eqs.(2), (9), (10), (11) and (12). Another one equation is determined through the mode of the pebble motion.

<u>Motion caused by rotation</u>

When the motion is caused by purely rotation, then Eq.(13) relating θ_A, and w is used.

$$(a+b)\frac{d\theta_A}{dt} = aw \tag{13}$$

Equations (10) to (12) are also simplified as follows:

$$\frac{2}{5}M(a+b)\frac{d^2\theta_A}{dt^2} = k_1F^* - k_2F_S \tag{14}$$

$$\frac{d^2\theta_A}{dt^2} = \frac{5}{7M(a+b)}\left\{R_T\cos(\alpha - \theta_A) + (R_L - W_g)\sin(\alpha - \theta_A) + k_1F^*\right\} \tag{15}$$

$$k_2F_S = k_1F^* - \frac{2}{5}M(a+b)\frac{d^2\theta_A}{dt^2} \tag{16}$$

When F_S is smaller than μN_A, the motion due to rotation takes place. This condition is expressed by Eq.(17).

$$F_S \leq \mu N_A \tag{17}$$

<u>Motion caused by rotation and sliding</u>

When the pebble moves by rotation and sliding, F_S is expressed by Eq.(18).

$$F_s = \mu' N_a \tag{18}$$

where μ' is the friction factor in motion.

In this case, equations of motion in horizontal and vertical direction are rewritten as follows:

$$\frac{d^2\theta_A}{dt^2} = \frac{1}{M(a+b)}\left\{R_T\cos(\alpha-\theta_A)+(R_L-Wg)\sin(\alpha-\theta_A)+k_2\mu' N_A\right\} \quad (19)$$

$$N_A = M(a+b)\left(\frac{d\theta_A}{dt}\right)^2 + R_T\sin(\alpha-\theta_A)-(R_L-Wg)\cos(\alpha-\theta_A) \quad (20)$$

The condition for the occurrence of motion due to rotation and sliding to take place is expressed as shown here.

$$F_S \le \mu N_A \ , \ (a+b)\frac{d\theta_A}{dt} \ne aw \quad (21)$$

When N_A becomes less than 0, the pebble leaps out.

These equations of motion are solved step by step by 4th-order Runge-Kutter method to obtain θ_A, v, w and so on. Before calculating these values, the mode of the motion are judged. In this case, there are 5 modes of the motion. That is, motion to left hand side and to right hand side, and the motion caused by purely rotation and that caused by rotation and sliding and no movement.

Using calculated values of θ_A and so on, variables concerning the pebble motion such as the horizontal displacement X, speed of displacement v and angular velocity ω are calculated according to the mode of motion.

Displacement caused by rotation:

$$X = (a+b)\left\{\sin\alpha - \sin(\alpha-\theta_A)\right\} \quad (22)$$

$$w = \frac{a+b}{a}\frac{d\theta_A}{dt} \quad (23)$$

$$v = (a+b)\frac{d\theta_A}{dt} \quad (24)$$

Displacement caused by rotation and sliding:

$$X = (a+b)\left\{\sin\alpha - \sin(\alpha-\theta_A)\right\} \quad (25)$$

$$w_n = \frac{5(k_1\mu^* - k_2\mu')}{2Ma}N_A h + w_{n-1} \quad (25)$$

$$v = (a+b)\frac{d\theta_A}{dt} \quad (25)$$

where subscript n and n-1 are the time steps of calculation.

When the pebble moves to the right hand side, the same modeling as shown above is done.

Evaluation of fluid force:

Figure 13 is the procedure for evaluating fluid force on the projective pebble. At first, wave field is determined by solving an equation of wave energy conservation, where the effect of bottom permeability is taken into account. Then the wave-induced current is calculated by solving depth and time averaged shallow water equations. Spatial and temporal variation of fluid motion caused by waves is assumed to be sinusoidal.

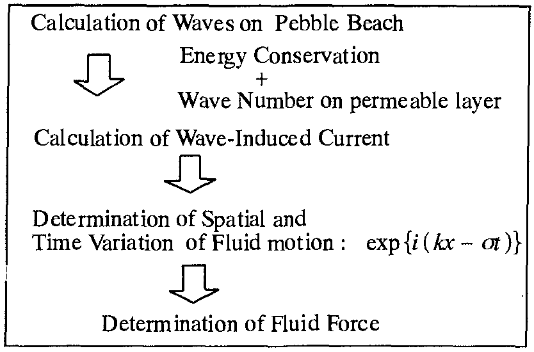

Fig. 13 Flow for determining fluid force

Finally the spatial and temporal variation of fluid force on pebble are determined by Eq.(26) where C_D is the drag coefficient and is evaluated by Eq.(27), C_M is the added mass coefficient and $\mathbf{u_f}$ is the velocity vector due to waves and wave-induced current.

$$R_T = \frac{\rho_f C_D}{2}\frac{\pi D^2}{4}\left|u_f - u_s\right|\left(u_f - u_s\right) + \frac{\rho_f C_M}{2}\frac{\pi D^3}{6}\frac{d}{dt}\left(u_f - u_s\right) \qquad (26)$$

$$C_D = 2 + 24/R_e, R_e = \left|u_f - u_s\right|D/\nu \qquad (27)$$

In the following calculation, the vertical force is assumed to be negligibly small.

CALCULATED PEBBLE MOTION ON INITIAL PROFILE

These equations are extended to three-dimensional motion. In the actual beach, there are various arrangement of projected pebble. For simplicity, we assume the situation where the pebble is on uniformly arranged pebble layer. Then there are two initial arrangements of projected pebble as shown in Fig.14. We carried out calculations of the motion on these two initial conditions.

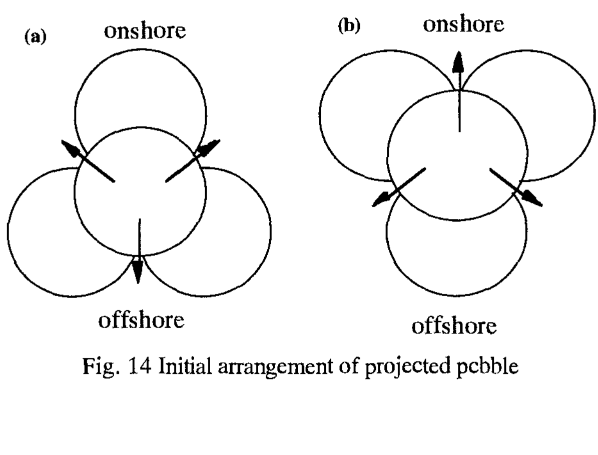

Fig. 14 Initial arrangement of projected pebble

As the first step of the application of these procedure, we calculated pebble motion on the initial beach with the straight parallel bottom contours. Figure 15 is an example of calculated wave field and wave-induced current under the condition of incident wave height is 1.2m , period is 4.5s and wave direction is 150°.

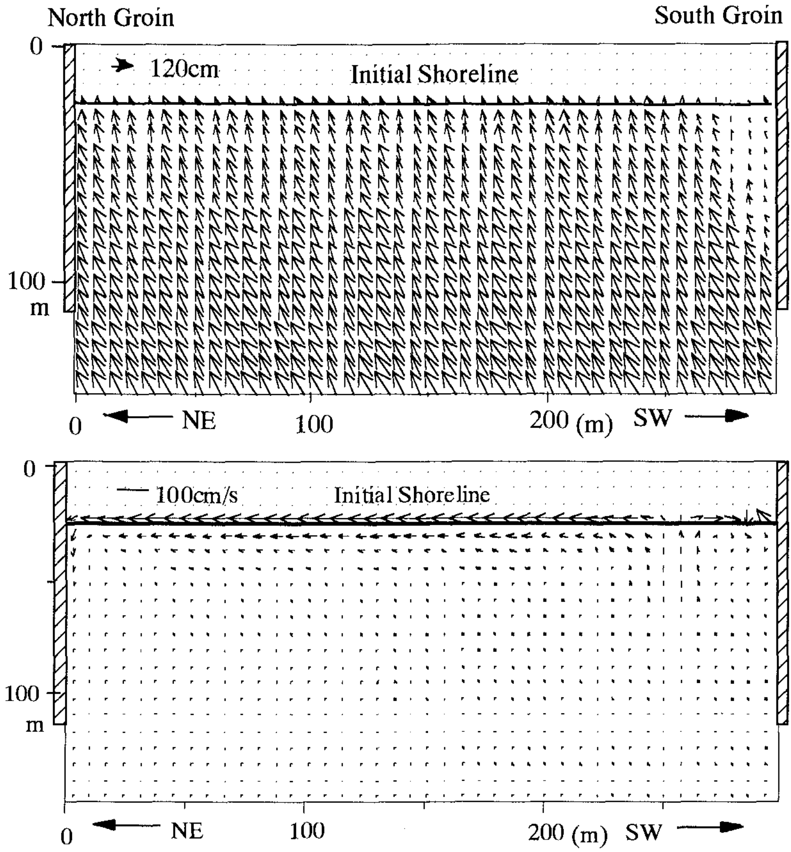

Fig. 15 Waves and wave-induced current on initial profile
(H_i=1.2m, T=4.5s, θ=150°)

Figure 16 is the examples of the calculated displacement of pebbles of diameter 6 cm during one wave period under the condition of fluid motion shown in Fig.15. The results shown by the thick line thin line correspond to the initial condition of the cases(a) and (b), respectively. Figure 17 is the result calculated under the small wave incidence.

Calculated results shown in Fig.16 indicates that the pebbles of diameter 6cm moves in the longshore direction toward NE. The maximum displacement takes place around the midpoint between shoreline and wave breaking point at the depth between 40cm and 60cm regardless of the initial condition. The maximum speed is 8cm/1cycle. When this waves continue for one half hour, the displacement of the pebble reaches almost 30m. The order of the displacement corresponds to the measured maximum displacement.

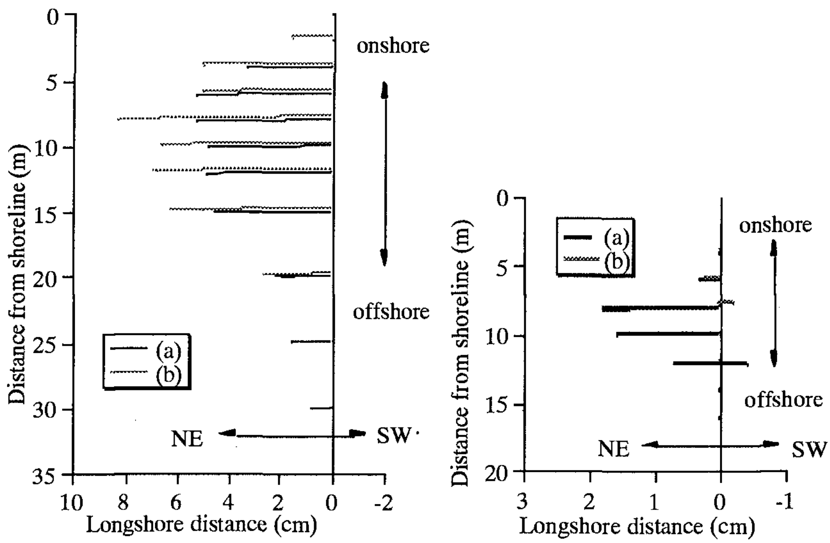

(a) H_i=1.2m, T=4.5s, θ=150^o (b) H_i=0.8m, T=4.5s, θ=150^o

Fig.14 Calculated displacement of pebbles during one period

The calculated speed of the same pebble at the same depth under the incident wave condition of wave height 80cm, period 4.5s and incident angle 150^o decreases significantly to 1cm/1cycle at the maximum. Any significant residual displacement is not calculated when wave height is 50cm.

By carrying out series of calculations of the movement of pebbles, we evaluated the rate of longshore pebble transport. It is found that the longshore pebble transport rate is not directly proportional to the longshore component of the incident wave energy flux at wave breaking point as is the case of the longshore sediment transport rate. The reason is explained by the difference of the characteristics of the movements of sand and pebble. The pebble usually moves intermittently during one wave period even under the condition of large wave incidence. While sand moves constantly over a whole wave period and is easily transported by wave-induced current when it is brought into suspension.

The movement of pebbles in the swash zone can not be reproduced by the numerical model because the model is based on the linear wave theory.

CONCLUSIONS

The main results obtained in this study are summarized as follows:

Pebbles on the surface of the beach of almost equilibrium profile move mainly in the longshore direction under obliquely incident waves.

The motion of pebble up to the maximum wave set-up point can be predicted numerically when the time and spatial variation of water particle velocity and fluid force on pebbles are given.

To evaluate the motion of pebbles in the swash zone, we have to solve a nonlinear wave equation including swash oscillation exactly.

REFERENCE

Araki S., S. Ito and I. Deguchi (1996): Equilibrium profile of rubble mound breakwater from the view point of dynamic response, Proc. Coastal Engineering, JSCE, Vol.43(2), pp.826-830.

Deguchi, I., M. Ono and T. Sawaragi (1996) :Wave on pebble beach and deformation of pebble beach, Proc. 25th Conf. Coastal Engineering, ASCE, Vol.3, pp.3349-3362.

Sawaragi, T. and I. Deguchi (1992) : Waves on permeable layer, Proc. 23 ICCE, ASCE, Vol.2, pp.1531-1544.